Mon. Not. R. Astron. Soc. **000**, 000–000 (0000) Printed 1 February 2008 (MN LATEX style file v1.4)

Lyα absorption in the nearby universe: the sightline to Q1821+643

David V. Bowen[1], Max Pettini[2], and Brian J. Boyle[3]

[1] *Royal Observatory, Edinburgh, Blackford Hill, Edinburgh EH9 3HJ*
[2] *Royal Greenwich Observatory, Madingley Rd., Cambridge CB3 0EZ*
[3] *Anglo-Australian Observatory, P.O. Box 296, Epping, NSW 2121, Australia*

Recieved 23 July 1997; accepted 10 December 1997

ABSTRACT

We present the first results of a survey designed to understand the origin of the Lyα-forest absorption systems at low redshift. Using the WYFFOS and HYDRA multi-fibre spectrographs on the WHT and WIYN telescopes, we have identified 51 galaxies brighter than $b_j = 18.5$ within 30 arcmins of the sightline of the QSO 1821+643. We find three galaxies within 500 h^{-1} kpc of the QSO sightline; the nearest galaxy is 104 h^{-1} kpc away from the line of sight, and is at the same redshift as a strong ($W_r = 0.63$ Å) Lyα absorption line. The remaining two galaxies have no corresponding absorption to extremely low equivalent width limits (< 0.05 Å). Beyond 500 h^{-1} kpc Lyα absorption lines are found at similar redshifts as several galaxies, but we show that these coincidences are likely to be accidental.

Half of the Lyα systems for which we could have found at least an L^* galaxy have no galaxies at the absorbers' redshifts. For the majority of the remainder, we show that any apparent association with galaxies is probably coincidental. These Lyα systems are characterised by their weak equivalent widths ($W_r < 0.2$ Å), and we conclude that this population of absorbers is uncorrelated, or at best, weakly correlated, with galaxies.

Key words: quasars: absorption lines — galaxies: haloes — cosmology: large-scale structure of the Universe

1 INTRODUCTION

Until recently, it was widely believed that the numerous, diffuse H I clouds which give rise to the dense Lyα-forest lines seen in high-redshift QSO spectra are *intergalactic* clouds not directly associated with galaxies (Sargent et al. 1980). However, since the launch of *HST* and the subsequent discovery of Lyα lines in the UV at redshifts < 1 (Bahcall et al. 1991; Morris et al. 1991), our understanding of their origin has become somewhat confused. The low-redshifts of these newly identified systems have made it possible to directly search for galaxies which may be responsible for the absorption, and deep CCD images of fields around observed QSOs, combined with spectroscopic confirmation of candidate galaxies, initially suggested that Lyα clouds are only weakly associated with galaxies on scales of $\sim 0.5 - 1$ Mpc (Morris et al. 1993, hereafter M93; Stocke et al. 1995). Later studies, however, found that most luminous galaxies at $0.1 < z < 1$ are apparently surrounded by extended gaseous envelopes $\sim 160\, h^{-1}$ kpc in radius* and that the fraction of Lyα-forest lines which occur in galaxies is high, between $\sim 40-70$ % (Lanzetta et al. 1995, hereafter LBTW). Confusingly, a study identical in method and objective, but using different sightlines, failed to confirm this result (Le Brun et al. 1996) and instead suggested that Lyα lines may simply follow the large scale structures which the brightest galaxies map out. More recent observations have shown that at least some Lyα absorbers reside in galaxy voids (Shull et al. 1996), although what that fraction is remains unclear.

In a previous paper (Bowen, Blades, & Pettini 1996; hereafter BBP) we conducted a search for Lyα absorption lines from *nearby* galaxies, since it is easier to study the origin and characteristics of Lyα clouds in the local universe. We concluded that nearby galaxies do not possess Lyα-absorbing halos beyond $\simeq 300\, h^{-1}$ kpc, and that *if* ab-

* $h = H_0/100$, where H_0 is the Hubble constant, and $q_0 = 0.5$ throughout this paper

sorption systems were directly associated with chosen galaxies, then $\sim 40\%$ of galaxies had absorbing halos of radii $50 - 300\ h^{-1}$ kpc. However, several facts led us to question whether galaxies we identified were actually responsible for a Lyα line when absorption was found, and we proposed that the most likely explanation was that absorbers follow the large-scale structure of the galaxy distribution, a conclusion similar to that drawn by Le Brun et al. (1996) at higher redshift and supported by numerical simulations of the high redshift universe (e.g. Cen et al. 1994; Petitjean, Mücket & Kates 1995; Zhang et al. 1995; Mücket et al. 1996). An alternative explanation is that Lyα absorbers are associated with dwarf galaxies or low surface-brightness galaxies; in that case the bright galaxies we had selected which appeared to show absorption were not in fact directly responsible for the absorption. A similar suggestion has been made by Shull et al. (1996).

The observations reported in BBP were designed to study the incidence of absorption in galactic halos; we did not, however, quantify the fraction of the Lyα-forest associated with galaxies. To determine this quantity, complete redshift information must be obtained in the field of a QSO sightline to ensure that any galaxy which might be associated with any particular absorption line could be detected — at least to some limiting magnitude.

We have therefore begun a spectroscopic survey of galaxies in fields of selected QSOs observed with *HST* in the far UV, to characterise any association of Lyα absorption systems with present day galaxies and their large scale structure. With the advent of multi-fibre spectrographs able to obtain redshifts of relatively faint galaxies over large areas of sky, it is now feasible to pursue such a study. In this paper we present the first results of our programme, identification of a magnitude limited sample of galaxies toward the bright QSO 1821+643 ($z_{\rm em} = 0.297$). This was one of the first QSOs to be observed with *HST* (Bahcall et al. 1992), and was one of the sightlines studied by Le Brun et al. (1996) in order to identify intermediate-redshift Lyα absorbers. Q1821+643 is unique in being one of the few QSOs bright enough to be observed with the Faint Object Spectrograph (FOS) aboard *HST and* the medium resolution gratings of the Goddard High Resolution Spectrograph (GHRS). This means that over small wavelength regions it is possible to search for weak Lyα lines (equivalent widths < 100 mÅ) which cannot be seen in FOS data.

This paper is structured as follows: In §2.1 we present spectra of galaxies obtained with the multi-fibre spectrographs WYFFOS/AF-2 attached to the William Herschel Telescope (WHT) on La Palma, and HYDRA on the WIYN telescope at the Kitt Peak National Observatory. §2.2 discusses our re-analysis of the avilable *HST* data. In §3 we present the results from our survey, and discuss the size of individual galaxy halos (§3.1) and the association of Lyα lines with galaxies in general (§3.2). In §3.3 we consider whether the associations found are significant compared to a random distribution of galaxies and absorbers. Our conclusions are summarised in §3.5.

2 OBSERVATIONS

2.1 Galaxy redshifts

2.1.1 WYFFOS data

Lists of galaxy candidates were produced from a scan of the POSS-II plate PJ3948c which covers the field of Q1821+643 using the Automated Plate Measuring (APM) Scanning Machine in Cambridge. The majority of spectra were obtained with the WYFFOS/AF-2 instrument on the WHT on August 20 and August 22nd 1995. WYFFOS is a bench spectrograph situated at the Nasmyth platform of the WHT, fed by 2.7 arcsec fibres positioned at the prime focus of the telescope using the Autofib-2 fibre positioner, with a circular field of view of 30 arcmins radius. Data were obtained using the R600B grating centered at 5200 Å and a thinned Tektronix 1024 CCD as the detector giving a wavelength coverage of ≈ 3000 Å.

Fibre configurations were produced using the `configure` routine, with priority given to the brightest objects in our sample. With a configuration completed, objects already allocated with a fibre were removed from the list, and the configuration routine run again, with the same magnitude priority acting on the list to produce the next configuration. Two exposures of 1200 sec were taken at each fibre configuration. Fibres unallocated to galaxy candidates were used for obtaining sky spectra, and wavelength calibration frames were taken for each fibre configuration. To maximise the efficiency of the available telescope time, we decided to obtain spectra of all objects with APM magnitudes of $b_j \leq 18.5$ in the 30 arcmin radius field of view. Spectra were obtained of 69 objects using 3 fibre configurations. These objects are listed in Table 1, with object designation given in column 1. The nomenclature of objects is arbitrary, but the EXT designation indicates objects which were not selected from the APM scans as galaxies, but were nevertheless added either because their classification as galaxies were marginal or because of their proximity to the QSO sightline. All these objects turned out to be stars.

Data were reduced using the `wyffos` data reduction package (Lewis 1996) running under IRAF. Redshifts of extracted spectra were measured by cross-correlation with two radial velocity standards HD182572 ($v_r = -100.5 \pm 0.4$ km s^{-1}) and HD171391 ($v_r = +6.9 \pm 0.2$ km s^{-1}) using the `rv` IRAF package. The resolution of our data, as measured from the calibration arc lines, was 6.2 Å, or 350 km s^{-1} at 5300 Å; cross-correlation of galaxy spectra with template radial standards is known to give accuracies of $\sim$ 0.1$\times$ FWHM, or $\sim$ 35 km s^{-1} for our data. Cross correlation of the two radial velocity standards with each other easily found the correct shift, confirming that the technique could certainly measure velocities to at least 100 km s^{-1}.

Sky was subtracted from each spectrum using summed sky spectra obtained during object exposures. Column 6 of Table 1 indicates the quality of the final spectrum: 'a' indicates a certain redshift, measured independently from both of the two exposures of a given fibre configuration; 'b' also indicates a certain redshift (more than one feature is identified in a spectrum) but the redshift could only be measured accurately from one of the exposures; 'c' means a redshift could be measured but the data were of low quality and the redshift may be uncertain (this applied to only two ob-

jects in our sample); 'd' indicates that no redshift could be measured.

Of 69 objects observed, 63 redshifts were obtained. Of these, 44 were galaxies. Redshifts for 68 objects are given in column 5 of Table 1 (Obj56 in the original list of 69 objects measured was removed — see §2.1.2), along with the RA & DEC of the object (cols. 2 and 3), the b_j magnitude derived from the APM scans (col. 4), the angular separation of the object on the plane of the sky from the QSO, θ, in arcmins, (col. 7), and the corresponding separation in units of h^{-1} kpc, ρ, when the redshift is known. Values of $\rho = 0$ are given for objects identified as stars.

2.1.2 HYDRA data

Additional spectra of objects in the field of Q1821+643 were obtained with the HYDRA instrument on the WIYN telescope at Kitt Peak. HYDRA is similar in design to WYFFOS in that a fibre positioner feeds optical fibres to a bench spectrograph. The field of view (30 arcmin radius) is also the same. Observations were made as part of the WIYN Queue Observing Experiment on September 3rd 1996 using 316 lines mm^{-1} grating centered at 5800 Å and a thinned 2048x2048 CCD covering a wavelength range of ≈ 4000 Å.

Three exposures of 2400 sec each were taken with one fibre configuration. Fibres unallocated to galaxy candidates were again used for obtaining sky spectra, and wavelength calibration frames were taken before and after the configuration exposures. Data were reduced using the `dohydra` data reduction package (Valdes 1992) running under IRAF. Redshifts of spectra were measured by cross-correlation with the same two radial velocity standards used for the WYFFOS data. The resolution as measured from the comparison arc lines was 8.4 Å, or 430 km s^{-1} at 5800 Å.

Spectra were obtained of 80 objects. 58 of these had already been observed with WYFFOS. Several HYDRA spectra yielded redshifts which could not be be measured in the WYFFOS data. These objects, as well as those not covered by the WYFFOS configurations, are listed separately in Table 1. For objects with redshifts identified from both sets of data, only one galaxy was found to have a discrepant redshift. This galaxy (Obj56 in Table 1) was one of the two spectra with a 'c' quality flag in the WYFFOS data, and we adopt the HYDRA measurement of its redshift in Table 1.

2.1.3 Completeness

As noted above, our initial goal was to observe all galaxies within 30 arcmins of the sightline of Q1821+643 down to a magnitude of $b_j = 18.5$. Combining the WYFFOS and HYDRA data, we measured 68 of 71 galaxy candidates, a completeness of 96%. 17 of 68 candidates, or 25%, were found to be stars. A large number of stellar spectra were expected, since we included objects marginally identified as galaxies to ensure that compact galaxies were not exlcuded in our sample. The distribution of confirmed galaxies in Right Ascension and Declination vs. redshift is shown in Fig. 1. We believe the errors in the APM magnitudes may be within ± 0.5 mags, but CCD images taken over the entire field of view of the spectrographs are needed to confirm this figure. Thus, the total galaxy sample considered here consists of 51 galaxies brighter than $b_j = 18.5$ within 30 arcmin of Q1821+643 on the plane of the sky.

2.2 Identification of Lyα systems

There exist several independent observations of Q1821+643 made with *HST*, covering different wavelength ranges and obtained at different resolutions. The first data were obtained with the *FOS* by Bahcall et al. (1992, hereafter B92) using the G130H, G190H, and G270H gratings, and subsequently reanalysed as part of the Absorption Line Key Project (Bahcall et al. 1993, hereafter KPI). Higher resolution data from the GHRS were obtained by Savage, Sembach & Lu (1995, hereafter SSL) with the G160M grating over two small wavelength regions from $1232 - 1269$ Å and $1521 - 1558$ Å. Finally, GHRS G140L data are available from the *HST* Archive, taken 30-March-1996 and covering the wavelength range $\simeq 1255 - 1530$ Å.

Comparing the list of Lyα absorption lines identified in FOS spectra by B92 and KPI shows several inconsistencies which arise from changes in their method of line identification. Further, the high resolution GHRS spectra obtained by SSL show that some of the initial identifications in the FOS spectra were erroneous. To derive a list of Lyα absorption systems to compare with galaxies detected in our spectroscopic survey, we have extracted the FOS and GHRS data from the *HST* Archive and reanalysed the data with our own software. Our identification of absorption lines follows similar procedures to those described by Young et al. (1979) and by B92. (These procedures differ from those used subsequently by KPI who used the instrumental Line Spread Function (LSF) of the spectrograph to weight the summation of pixels comprising a line in the determination of its equivalent width.)

There are several differences in our analysis to those used by B92 and KPI. First, we have corrected the FOS wavelength scales by applying a shift to match the rest wavelengths of low ionization lines arising from Galactic absorption in the spectra to the velocity of the bulk of H I emission measured at 21 cm. We take the heliocentric velocity of this gas to be at $\simeq -40$ km s^{-1} (Lockman & Savage 1995). Second, no accurate LSFs are available for the FOS aperture used ($0\farcs25 \times 2\farcs0$) so we have not used an LSF to estimate the equivalent widths of lines. Instead, we have taken the number of pixels over which an absorption feature is detected to be 11. This, for example, is the extent of the LSF for the $1\farcs0$ aperture (see BBP). Third, error arrays supplied by the pipeline wavelength calibration of FOS spectra do not include any contribution from the background or from other sources such as scattered light, and are therefore inadequate for determining the reality of a feature in a spectrum. We have therefore constructed arrays from measured rms deviations in regions of a spectrum clearly free of absorption lines, and used these for our error arrays. The flux arrays used to measure the noise are those prior to the data being resampled to a linear wavelength scale because resampling introduces a smoothing of the flux. For GHRS data, the pipeline calibrated error arrays are true representations of the noise in the data, and can be used for detection and measurement of absorption lines.

Our final line lists consist of lines at wavelength $\lambda_{\rm obs}$, with observed equivalent widths, W, which are $\geq 3\sigma(W)$,

Table 1. Galaxy Redshifts within 30′ of Q1821+643

Des	RA (J2000.0)	Dec	b_j	$z_{\rm gal}$	Qual.	θ (′)	ρ (h^{-1} kpc)
			WYFFOS data				
Ext	18:25:12.31	+64:30:04.8	16.77	−0.00040	a	23.10	0.0
Obj81	18:23:58.30	+64:26:51.3	14.45	0.12311	a	14.50	1269.9
Obj19	18:25:26.87	+64:36:39.1	18.14	...	e	27.71	...
Obj54	18:24:40.36	+64:34:54.0	17.00	0.10642	a	22.67	1761.9
Obj39	18:25:04.56	+64:40:35.8	18.32	0.09583	a	28.39	2020.8
Obj58	18:24:33.84	+64:38:51.2	14.82	...	e	24.85	...
Obj113	18:23:15.55	+64:33:05.6	17.78	0.19188	b	15.08	1854.1
Obj93	18:23:38.88	+64:41:46.7	12.71	0.08826	a	23.83	1581.3
Obj153	18:22:20.92	+64:26:50.9	17.17	0.19231	a	6.75	831.2
Obj144	18:22:31.70	+64:35:28.4	12.90	0.05047	a	15.33	618.9
Obj142	18:22:36.11	+64:45:44.9	16.41	...	e	25.49	...
Obj167	18:22:07.61	+64:39:32.4	17.47	0.05039	a	18.97	764.8
Obj186	18:21:49.21	+64:37:48.4	10.08	0.05019	a	17.22	691.7
Obj198	18:21:36.70	+64:45:22.6	17.09	0.10725	a	24.87	1945.4
Obj216	18:21:21.38	+64:49:40.4	18.08	...	e	29.32	...
Obj219	18:21:18.20	+64:43:35.5	18.19	−0.00008	a	23.37	0.0
Obj264	18:20:14.22	+64:38:56.5	16.50	−0.00018	a	21.42	0.0
Obj238	18:20:56.96	+64:27:55.0	17.52	0.07198	a	9.78	543.5
Obj293	18:19:40.64	+64:30:38.5	17.92	0.17955	a	17.83	2089.2
Obj318	18:18:53.04	+64:30:37.4	18.47	−0.00009	a	22.25	0.0
Obj290	18:19:44.59	+64:23:07.4	15.66	0.08941	a	14.56	977.0
Obj334	18:18:14.83	+64:18:22.4	16.95	0.05106	a	24.19	987.1
Obj272	18:20:02.47	+64:18:53.0	18.32	0.02788	a	12.54	290.5
Obj332	18:18:17.71	+64:16:15.9	17.41	0.18002	a	24.18	2838.7
Obj338	18:18:02.25	+64:14:04.2	16.91	0.12103	a	26.30	2271.7
Obj327	18:18:35.45	+64:14:20.8	16.49	0.09538	a	22.75	1612.9
Obj245	18:20:48.75	+64:18:52.4	18.29	−0.00029	a	7.61	0.0
Obj307	18:19:24.44	+64:07:53.1	17.85	0.17993	a	20.91	2453.9
Obj221	18:21:19.80	+63:59:45.2	16.86	−0.00015	a	21.25	0.0
Obj146	18:22:30.82	+64:04:12.9	15.41	0.07171	a	16.79	929.9
Obj137	18:22:41.28	+64:10:27.1	17.07	...	e	11.23	...
Obj112	18:23:16.01	+64:04:52.9	14.11	0.02754	a	17.91	410.0
Obj92	18:23:41.16	+64:01:08.3	16.70	0.07249	a	22.52	1259.2
Obj213	18:21:25.88	+63:51:36.0	17.22	0.00028	a	29.21	0.0
Obj204	18:21:37.94	+63:51:24.4	18.01	0.00070	b	29.27	0.0
Obj178	18:21:57.41	+63:52:44.1	17.00	0.00004	a	27.87	0.0
Obj165	18:22:09.95	+64:09:36.9	17.87	0.08410	a	11.08	705.3
Obj151	18:22:25.74	+63:53:51.5	18.46	0.00005	a	26.93	0.0
Obj105	18:23:25.41	+64:08:34.0	9.38	0.05033	a	15.39	619.8
Obj53	18:24:40.55	+64:02:45.1	17.09	0.09681	a	25.20	1809.2
Obj67	18:24:21.54	+64:06:26.2	7.30	0.05106	a	21.14	862.6
Obj34	18:25:08.16	+64:09:17.3	18.37	0.13853	a	23.63	2273.5
Obj15	18:25:46.41	+64:07:56.8	18.22	0.07200	b	27.94	1553.0
Obj63	18:24:28.05	+64:16:41.5	17.98	0.08470	c	16.81	1076.7
Obj172	18:22:02.73	+64:21:38.7	17.60	0.12160	a	1.20	104.0
Obj217	18:21:22.44	+64:28:28.7	18.08	0.12245	a	8.72	760.4
Obj180	18:21:53.90	+64:19:49.8	18.34	−0.00012	a	0.85	0.0
Obj345	18:17:33.14	+64:19:29.9	17.38	0.00000	b	28.61	0.0
Obj271	18:20:04.95	+64:19:44.3	18.47	−0.00014	a	12.18	0.0
Obj242	18:20:53.45	+64:19:37.1	18.10	0.11155	b	6.97	563.2
Obj212	18:21:25.61	+64:02:11.0	17.79	0.19406	a	18.74	2322.7
Obj192	18:21:41.26	+63:51:37.2	15.81	0.02380	b	29.04	578.4
Obj132	18:22:47.01	+63:59:28.6	15.49	0.07201	a	21.82	1213.0
Obj140	18:22:36.32	+64:12:42.1	17.96	−0.00034	a	8.97	0.0
Obj57	18:24:33.26	+64:16:13.9	16.63	0.05305	a	17.48	738.6
Obj72	18:24:12.74	+64:24:40.1	18.02	−0.00011	a	15.21	0.0
Obj97	18:23:34.34	+64:18:35.1	17.01	0.05099	a	10.72	436.9
Ext	18:24:09.55	+64:19:33.7	18.17	−0.00035	a	14.37	0.0

Table 1. Cont.

Des	RA (J2000.0)	Dec (J2000.0)	b_j	$z_{\rm gal}$	Qual.	θ ($'$)	ρ (h^{-1} kpc)
Obj10	18:26:01.05	+64:23:16.4	16.17	0.07623	a	26.51	1549.3
Obj73	18:24:12.45	+64:35:12.7	18.24	−0.00020	a	20.64	0.0
Obj90	18:23:42.40	+64:32:53.3	16.81	0.05242	a	16.72	698.8
Obj87	18:23:44.90	+64:42:45.9	18.06	0.08849	a	25.00	1662.7
Obj148	18:22:29.27	+64:41:05.4	16.76	0.08807	a	20.77	1375.7
Obj347	18:17:26.18	+64:19:43.7	18.24	...	e	29.35	...
Obj230	18:21:08.73	+63:52:09.0	18.04	0.15039	a	28.94	2968.2
Obj118	18:23:09.33	+63:52:23.4	17.14	0.00000	a	29.29	0.0
Obj138	18:22:40.55	+64:09:43.7	18.42	0.12050	a	11.85	1019.9
Obj130	18:22:50.78	+64:09:40.8	18.40	0.00000	b	12.38	0.0
			HYDRA data				
Ext	18:23:57.96	+64:11:07.7	8.61	−0.00014	a	16.18	0.0
Obj131	18:22:50.92	+64:09:19.8	12.71	0.05086	a	12.70	516.4
Obj56	18:24:34.11	+64:19:04.1	14.80	0.05050	a	17.07	689.5
Obj58	18:24:33.84	+64:38:51.2	14.83	0.09605	b	24.85	1772.2
Obj181	18:21:52.77	+64:38:59.5	15.32	0.05050	a	18.39	742.9
Obj142	18:22:36.11	+64:45:44.9	16.42	0.04970	a	25.49	1014.7
Ext	18:25:12.31	+64:30:04.8	16.77	−0.00030	a	23.10	0.0
Obj216	18:21:21.38	+64:49:40.4	18.08	0.05683	c	29.32	1318.9
Obj19	18:25:26.87	+64:36:39.1	18.14	0.09517	a	27.71	1960.9
Ext	18:24:09.55	+64:19:33.7	18.18	−0.00025	a	14.37	0.0
Obj347	18:17:26.18	+64:19:43.7	18.25	0.08210	b	29.35	1829.8
Obj62	18:24:29.09	+64:01:05.3	18.57	0.08420	a	25.58	1630.0
Obj13	18:25:53.58	+64:19:18.5	18.61	0.11159	b	25.63	2071.7
Obj309	18:19:23.46	+63:59:26.8	18.61	0.00005	a	26.98	0.0
Obj331	18:18:17.57	+64:34:37.2	18.65	0.07836	a	27.51	1647.0
Obj20	18:25:20.57	+64:16:35.7	18.67	0.09697	a	22.41	1611.2
Obj313	18:19:07.28	+64:36:50.3	18.67	...	e	24.46	...
Obj269	18:20:08.55	+64:00:06.1	18.71	0.00006	a	23.67	0.0
Obj241	18:20:57.82	+63:56:00.8	18.71	0.00040	a	25.43	0.0
Ext5	18:22:11.40	+64:28:43.0	18.77	−0.00013	a	8.26	0.0
Obj234	18:21:00.73	+64:37:54.3	18.77	0.26650	c	18.34	2813.8
Obj314	18:19:10.44	+64:07:27.4	18.77	0.09458	a	22.39	1576.1
Obj297	18:19:34.62	+64:42:21.0	18.77	0.16410	a	26.60	2915.55
Obj328	18:18:28.71	+64:38:03.6	18.80	0.16550	a	28.43	3136.0
Obj205	18:21:35.27	+64:25:24.0	18.83	0.18900	a	5.35	650.7
Obj38	18:25:04.35	+64:25:23.1	18.85	0.12005	a	20.79	1784.0
Obj275	18:19:56.14	+64:40:20.0	18.85	0.00008	a	23.64	0.0

where $\sigma(W)$ is the error in the equivalent width at $\lambda_{\rm obs}$. For lines which are in common with those found by B92 and KPI, the majority of our measurements of W are within $\pm 3\sigma(W)$ of their measurements. Hence our measurements of W give values close to those already published. Only if a line sits on the peak of an emission line do equivalent widths differ by more that $\pm 3\sigma(W)$, because errors inherent in continuum fitting around the emission line mean that the true value of $\sigma(W)$ is greater than that estimated from the noise. Of the 18 lines we detect in FOS or published GHRS data, 15 have been identified by B92, SSL, and/or KPI. We detect an additional Lyα line in the GHRS data at 1252.1 Å, which is weak, but present at the 3σ level in our analysis. Another two lines are marginal detections in the FOS G130H data, but are confirmed in the unpublished GHRS G140L spectrum.

The Lyα lines we identify are listed in Table 2. Column 4 lists the absorption redshift, $z_{\rm abs}$, of the absorption line; column 5, $z_{\rm GHRS}$, indicates whether the redshift has been determined from the high resolution G160M GHRS spectra of SSL, either by direct measurement of the Lyα line or higher order Lyman lines of the same absorption system. Measurements of $z_{\rm abs}$ using these spectra are more accurate than those derived from the FOS data. Column 6 lists the absolute magnitude we reach in our survey at $z_{\rm abs}$ given the limiting observed magnitude of $b_j = 18.5$. Column 7 lists in which spectra the lines have been identified, while in column 8 we record whether the authors mentioned above also identified the line.

We identify lines at 1264.2 and 1270.9 Å as Lyα absorption at redshifts of $z_{\rm abs} = 0.0399$ and 0.0454. However, it is also possible that these are actually an O VI absorption doublet at $z_{\rm abs} = 0.2249$, from an absorption system identified by its strong Lyα and Lyβ absorption (Tripp et al. 1997). We maintain that the lines are indeed low-redshift Lyα absorption for two reasons: a) the $z_{\rm abs} = 0.2249$ Lyβ and O VIλ1031 lines do not match up in velocity (although this could be because of additional lower column density gas which shows up in H I absorption but not O VI); and b) there is no absorption from C IV, Si IV or N V (or indeed from

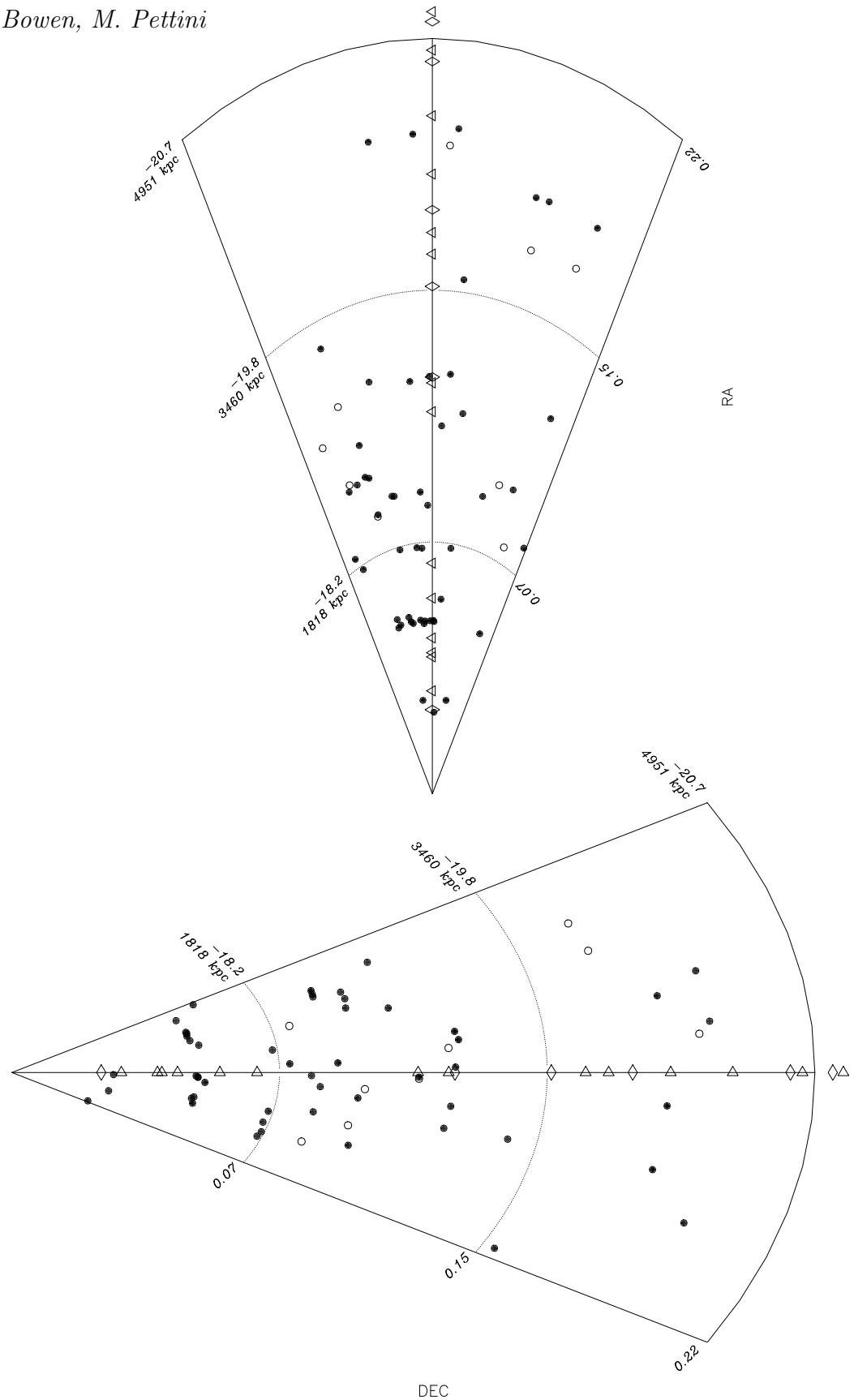

Figure 1. Wedge diagrams showing the spatial distribution of galaxies observed with WYFFOS and HYDRA as a function of redshift, plotted in RA (top) and DEC (bottom). Redshifts of Lyα lines towards Q1821+643 are plotted along the central axis; diamonds indicate lines with $W_r \geq 0.2$ Å, triangles $W_r < 0.2$ Å. Galaxies forming part of our magnitude limited sample of $b_j \leq 18.5$ are shown as filled circles, fainter galaxies are open circles. The absolute magnitudes of this limit at the redshifts marked along the right axis of each cone are shown on the left side, along with the comoving angular distance that 30 arcmin corresponds to at the same redshift.

Table 2. Lyα systems along the line of sight to Q1821+643

$\lambda_{\rm obs}$ (Å)	W (Å)	$\sigma(W)$ (Å)	$z_{\rm abs}$	$z_{\rm GHRS}$	$M_{\rm lim}$	Instr.[a]	Who else?[b]
1245.33	0.32	0.02	0.0245	y	−15.8	1	SSL
1252.10	0.05	0.02	0.0300	y	−16.3	1	
1264.17	0.19	0.02	0.0399	y	−16.9	1,3	SSL
1265.59	0.04	0.01	0.0411	y	−16.9	1	SSL
1270.9	0.13	0.01	0.0454	n	−17.2	2,3	
1285.0	0.06	0.01	0.0570	n	−17.7	2,3	
1297.3	0.13	0.01	0.0672	n	−18.1	3	KPI
1351.0	0.10	0.01	0.1113	n	−19.2	3	
1361.2	0.05	0.01	0.1197	n	−19.3	3	
1363.2	0.71	0.06	0.1214	n	−19.4	2,3	B92,KPI
1395.3	0.35:	0.06	0.1478	n	−19.8	2,3	B92,KPI
1406.8	0.06	0.01	0.1572	n	−19.9	3	
1414.4	0.07	0.01	0.1635	n	−20.0	3	
1422.5	0.62	0.06	0.1701	n	−20.1	2,3	B92,KPI
1435.1	0.23	0.06	0.1805	n	−20.3	2,3	KPI
1455.8	0.13	0.01	0.1975	n	−20.5	3	
1474.8	0.54	0.07	0.2133	y	−20.6	2,3	B92,KPI
1478.7	0.20	0.07	0.2166	y	−20.7	2,3	KPI
1489.3	1.01	0.07	0.2249	y	−20.8	2,3	B92,KPI
1492.6	0.16:	0.02	0.2278	n	−20.8	2,3	B92
1513.7	0.06	0.02	0.2452	n	−21.0	3	
1529.46	0.21	0.02	0.2581	y	−21.1	1,2,3	SSL,B92
1533.63	0.22	0.02	0.2616	y	−21.1	1,2	SSL,B92,KPI
1539.74	0.24	0.02	0.2666	y	−21.1	1,2	SSL,B92,KPI
1576.6	0.56	0.03	0.2967	y	−21.4	2	B92,KPI

[a] Line detected in — (1) GHRS G160M spectrum; (2) FOS G130H spectrum; (3) GHRS G140L spectrum
[b] Line also found by: SSL—Savage, Sembach & Lu 1995; B92—Bahcall et al. 1992; KPI—Bahcall et al. 1993

any other metal species) at $z_{\rm abs} = 0.2249$. Clearly, higher sensitivity observations are needed to test the identification of these lines further.

In Figs. 2 and 3 we show portions of the FOS G130H and GHRS G140L normalised spectra and Lyα systems identified. Comparisons between features found in both FOS G130H and GHRS G140L spectra suggest that the values of $z_{\rm abs}$ in Table 2 are consistent to within $|\Delta z| \approx 0.0002$.

2.3 NED galaxies

Due to the pencil-beam nature of our survey, the number of galaxies sampled below $z < 0.05$ begins to decline as the 1 degree angular size of the sky samples smaller physical radii, and hence volume. We have therefore supplemented our list of galaxies by searching the NASA Extragalactic Database (NED) for all galaxies with known redshifts within 300 arcmins of the QSO line of sight. Of 136 galaxies found, none were within 500 h^{-1} kpc of the QSO sightline. A wider search for galaxy clusters over 30 degrees revealed only two clusters close to the QSO sightline. ZwCl 1638.4+6038 at $z = 0.01634$ is 10.3 h^{-1} Mpc away, while Abell 2295 at $z = 0.05080$, is 13.0 h^{-1} Mpc from the line of sight. The 13 galaxies we found at $z \simeq 0.051 \pm 0.02$ in Fig. 1 are presumably members of a larger structure of which Abell 2295 is part.

3 DISCUSSION

Since the aim of our programme is to study the association of Lyα lines with low-redshift galaxies, we have detected very few galaxies beyond $z = 0.2$ (see Fig. 1). The magnitude limit of our survey ($b_j \leq 18.5$) means we become insensitive to galaxies fainter than L^* beyond $z \approx 0.1$. Deeper searches for galaxies close to the QSO line of sight include those by Schneider et al. (1992), who have detected several galaxies within one arcmin. Although most appear to be at similar redshifts to the QSO itself, one galaxy (labelled G in their Table 1, 73 h^{-1} kpc from the QSO sightline) is within 600 km s^{-1} of the $z_{\rm abs} = 0.2249$ and 0.2278 absorption systems. Also, Le Brun et al. (1996) have detected a galaxy (their #8) at a redshift of 0.1703, 266 h^{-1} kpc from the QSO line of sight, and close to the redshift of the $z_{\rm abs} = 0.1701$ system listed in Table 2. However, since these galaxies have been detected in surveys with different magnitude limits, survey completion, and extent on the sky than our own, we do not include them in our subsequent analysis.

3.1 Lyα-absorbing cross-section of individual galaxies

We begin first by considering the limits we can set on the size of individual galaxy halos from our data. Table 1 contains 49 galaxies within 2 h^{-1} Mpc of the QSO line of sight. For each galaxy at a separation ρ from the QSO sightline

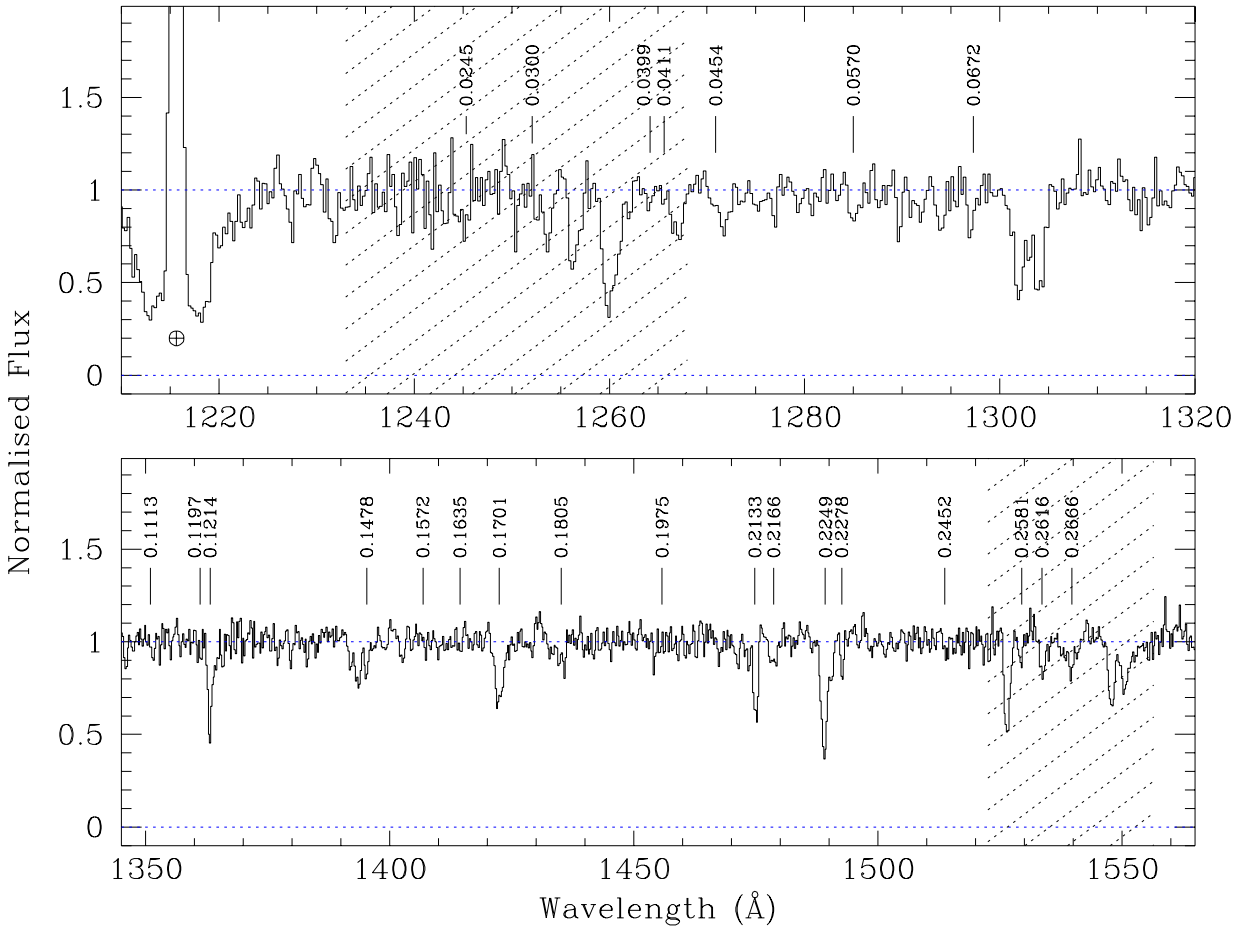

Figure 2. Portions of the normalised spectra of the FOS G130H spectrum of Q1821+643 originally presented by B92 & KPI. All the Lyα lines listed in Table 2 are indicated. The shaded regions represent wavelength ranges spanned by the high resolution GHRS G160M data obtained by SSL; tick marks which do not appear to correspond to any obvious lines here indicate the positions of weaker Lyα absorption revealed by GHRS G160M data. Similarly, lines marked between $\sim 1270 - 1320$ Å which appear marginal here can be seen in the GHRS G140L spectrum extracted from the *HST* Archive (Fig. 3).

we have searched for Lyα absorption in the QSO spectra within ± 600 km s^{-1} of the galaxy's measured redshift. 18 of these galaxies could not be searched for absorption, however, since any Lyα absorption which did arise at the redshift of the galaxy would be obscured by Milky Way absorption lines or other lines from higher redshift systems. Also, six galaxies would have Lyα absorption lines blended with the wings of weak ($W < 0.2$ Å) Galactic lines; in these cases it has only been possible to search for Lyα absorption from the galaxy within $\pm(200 - 300) \mp 600$ km s^{-1} of its velocity. Table 3 lists the first 13 galaxies within 1 h^{-1} Mpc for which we were able to search for absorption, and the detection of any Lyα lines. Δv given in column 7 is the velocity difference derived from $z_{\rm gal} - z_{\rm abs}$.

Fig. 4 plots ρ vs. W_r for galaxies where Lyα could be searched for; circles represent detections of Lyα absorption, limits are given by arrows. We find three galaxies within 500 h^{-1} kpc of the QSO line of sight, and detect Lyα absorption from the galaxy closest to the line of sight (Obj172) at $z_{\rm gal} = 0.1216$, $\rho = 104\ h^{-1}$ kpc. The absorption line is moderately strong, with a rest equivalent width of $W_r = 0.63$ Å, and there is no associated C IV absorption to 3σ equivalent width limits of 0.12 Å. The galaxy shows strong [O II], [O III], and Hβ emission, as well as strong Balmer lines, indicating recent star formation. However, the absorbing galaxies found by LBTW generally did not show emission lines, and it is unlikely that any correlation exists between the star formation implied by the spectral features in Obj172's spectrum and the existence of an extended gaseous halo.

The next closest galaxies are at impact parameters of 291 and 410 h^{-1} kpc; they show no absorption to extremely low equivalent width limits of 0.05 Å (their redshifts were covered by SSL's high resolution GHRS data; these data also show that no local Galactic lines prevent detection of Lyα at the galaxy redshifts). One other galaxy is within 0.5 h^{-1} Mpc, (Obj97 at $z_{\rm gal} = 0.05099$, $\rho = 437\ h^{-1}$ kpc)

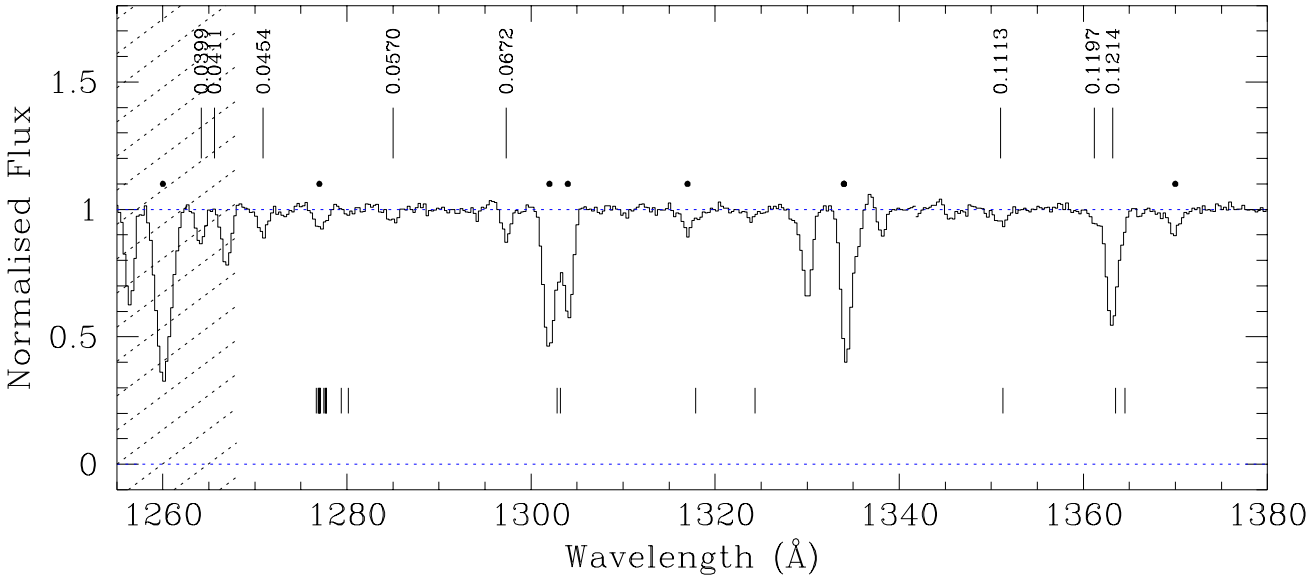

Figure 3. Portions of the normalised G140L spectrum extracted from the *HST* Archive, with the positions of Lyα lines marked. Data are binned at the original dispersion of 0.29 Å pix^{-1}. See caption to Fig. 2 for significance of shaded region. Redshifts of identified Lyα lines are shown above the spectrum, along with the positions of absorption lines from the Milky Way indicated by •; the expected wavelengths of Lyα absorption from all the galaxies listed in Table 1 which are within $\rho \leq 1\ h^{-1}$ Mpc are shown by tick marks below the spectrum.

Table 3. Galaxies with $\rho \leq 1\ h^{-1}$ Mpc from the sightline of Q1821+643

Des	$z_{\rm gal}$	$M_{\rm gal}$	ρ (h^{-1} kpc)	$z_{\rm abs}$	W_r (Å)	Δv (km s^{-1})
Obj172	0.12160	−20.3	104.0	0.1214	0.63	54
Obj272	0.02788	−16.3	290.5	...	< 0.05	...
Obj112	0.02754	−20.5	410.1	...	< 0.05	...
Obj242	0.11155	−19.6	563.2	0.1113	0.09	67
Obj192	0.02380	−18.5	578.4	0.0245	0.31	−205
Obj205	0.18900	−20.0	650.7	...	< 0.03	...
Obj90	0.05242	−19.2	698.8	...	< 0.03	...
Obj165	0.08410	−19.2	705.3	...	< 0.05	...
Obj57	0.05305	−19.4	738.6	...	< 0.03	...
Obj153	0.19231	−21.7	831.2	...	< 0.03	...
Obj67	0.05106	−22 :	862.6	...	< 0.10	...
Obj290	0.08941	−21.5	977.0	...	< 0.03	...
Obj334	0.05106	−19.0	987.1	...	< 0.10	...

but is not included in Fig. 4 or Table 3 because the redshift at which Lyα is expected is obscured by a weak line at 1277.1 Å which is probably Galactic C I. The line could in principle be Lyα at $z_{\rm abs} = 0.0505$, since there is no corresponding C Iλ1280. However, C Iλ1277 is detected in higher resolution GHRS data at roughly the same strength as observed here, and a simple Voigt profile fit to the C Iλ1277 line suggests that C Iλ1280 would be not be detected in spectra of the sensitivity of the G140L data. This is unfortunate, because the C Iλ1277 line obscures any Lyα absorption from the group of galaxies found at $z \sim 0.05$.

The detection of a single absorbing galaxy 104 h^{-1} kpc from the QSO line of sight is consistent with LBTW's conclusion that galaxies are surrounded by spherical halos of 160 h^{-1} kpc radius. There is good evidence from LBTW and BBP that individual galaxies are not surrounded by halos with radii greater than $\sim 200 - 300\ h^{-1}$ kpc, and although our data do not well sample galaxy halos on sizes $\rho = 100 - 500\ h^{-1}$ kpc, the data continue the trend of non-detections beyond $\rho = 500\ h^{-1}$ kpc, confirming that the majority of galaxies do not possess Lyα absorbing halos beyond 500 h^{-1} kpc. There are, however, a few cases

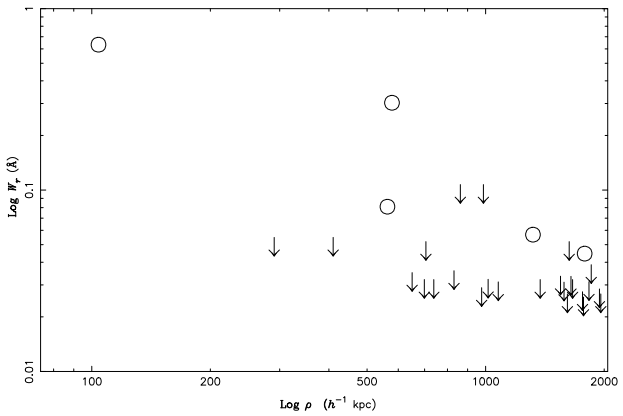

Figure 4. Plot of the distribution of ρ *vs.* rest equivalent width, W_r, for galaxies in our survey. Open circles represent detections of Lyα lines within $\Delta v = \pm 600$ km s^{-1} of a galaxy's velocity.

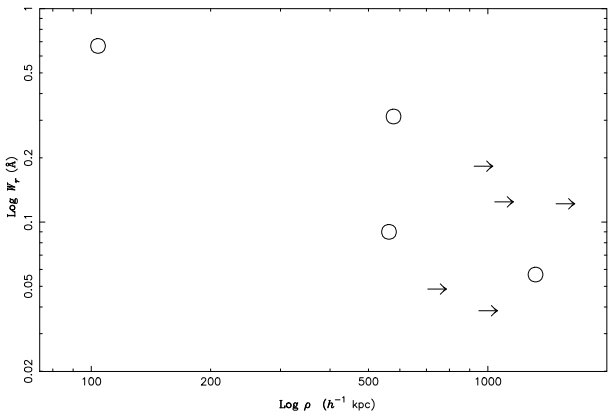

Figure 5. Plot of the distribution of rest equivalent width, W_r, of the Lyα lines towards Q1821+643, *vs.* impact parameters, ρ, of the nearest galaxies within $\Delta v = \pm 600$ km s^{-1} of the Lyα system. Open circles represent detections of a galaxy; lower limits correspond to the size that 30 arcmin corresponds to at the redshift of the absorption system.

where Lyα lines arise at the same redshifts as galaxies. This is similar to what BBP found on scales of $100-500\ h^{-1}$ kpc, where a few absorber-galaxy associations were found despite the general trend of non-detections. In that work, it was impossible to test whether those associations were statistically significant or not. Here, however, we have a controlled sample of galaxies and absorption systems which allows us to test whether the detection of Lyα at the same redshifts as galaxies is coincidental, although with our data we are mainly testing associations on scales of $> 200\ h^{-1}$ kpc.

Another important point to emphasise is that the majority of Lyα lines lines listed in Table 2 are weak, $W_r < 0.2$. These lines are not detectable in the FOS spectra of Q1821+643 [Bahcall et al. (1996) in their analysis of FOS Key Project data set a canonical value of 0.24 Å as the limit to which FOS spectra are sensitive over a large spectral range], and are only identified clearly in the more sensitive GHRS data. This makes it even more important to test whether apparent galaxy-absorber associations arise purely from chance, because the density of weak lines with redshift is very much higher than strong ones, increasing the chances of 'accidental' coincidence close to the line of sight. The statistical significance of all associations shown in Fig. 4 are discussed in detail in §3.3.

3.2 Association of Lyα-clouds with galaxies

In Table 4 we list the ten Lyα lines for which we could have detected a galaxy with luminosity brighter than $\approx L^*$, and any galaxies found within ± 600 km s^{-1} of the absorption line. The limit to ρ when no galaxy is found depends on the distance that 30 arcmins corresponds to at the redshift of a Lyα line; these lower limits are given in column 6, and range from $\simeq 0.75-1.6\ h^{-1}$ Mpc. Column 7 gives the proper separation, $s\ h^{-1}$ Mpc, between absorber and galaxy assuming that Δv represents cosmological (i.e. "Hubble Flow") distances. $M_{\rm lim}$ is again listed in column 8 to highlight the limit to which we are able to detect galaxies.

Of the ten Lyα lines listed in Table 4 we are unable to detect any galaxies at similar redshifts from five (50%) of them. This result is shown graphically in a plot of W_r vs. ρ for nine of the absorption systems in Fig. 5 (for this figure, we have assumed that the weak line at $z_{\rm abs} = 0.1197$, separated by 450 km s^{-1} from the $z_{\rm abs} = 0.1214$ line, is associated with the galaxy $104\ h^{-1}$ kpc from the QSO sightline). The figure suggests that at least half of the Lyα lines are intergalactic in origin. As mentioned above, eight of the ten Lyα lines are weaker than $\simeq 0.2$ Å; hence we are discussing a population of Lyα lines much weaker than those detectable in FOS spectra. Six of these eight weak absorbers have no bright galaxies at separations less than $(0.7-1.3)\ h^{-1}$ Mpc. There are two strong lines ($W_r > 0.3$ Å) at $z_{\rm abs} = 0.0245$ and 0.1214, and both have galaxies 578 and $104\ h^{-1}$ kpc from the QSO sightline respectively. Again, the question is whether these associations are coincidental, a question we attempt to answer in §3.3.

Our survey detects one obvious group of galaxies at $z \approx 0.05$ (see Fig. 1). As noted above, possible absorption by Lyα at this redshift is unfortunately obscured by a weak Galactic C I absorption line. It is clear though that strong Lyα absorption, with equivalent widths greater than the W(C Iλ1277) $\simeq$ 0.1 Å observed, is *not* associated with this group of galaxies. A direct association between galaxy groups and Lyα absorption systems has been claimed by Lanzetta et al. (1996) for a group of galaxies toward Q1545+2101 at $z = 0.26$; in their example, all five galaxies constituting the group are within $\rho = 500\ h^{-1}$ kpc of the QSO sightline, and the resulting Lyα absorption is strong ($W = 0.8$ Å) and broad. In our data, there are 12 galaxies in a redshift interval $0.04950 - 0.05250$ (which corresponds to depth of $8\ h^{-1}$ Mpc along the line of sight) but all are at separations of $\rho = 0.44 - 1.01\ h^{-1}$ Mpc. This clearly shows that loose groups of galaxies — where intracluster gas might be expected to produce absorption — need not produce Lyα absorption. M93 found a similar example towards 3C 273.

In contrast, there are three absorption lines at $z_{\rm abs} = 0.0399 - 0.0454$ (a depth of $\sim 15\ h^{-1}$ Mpc) which are offset from this galaxy group, and unassociated with any galax-

Table 4. Nearest galaxies to Lyα lines within 600 km s^{-1}

$z_{\rm abs}$	W_r (Å)	Des	$z_{\rm gal}$	Δv (km s^{-1})	ρ (h^{-1} kpc)	s (h^{-1} Mpc)	$M_{\rm lim}$
0.0245	0.31	Obj192	0.0238	−205	578.4	2.06	−15.8
0.0300	0.05		*no galaxy*		> 745	...	−16.3
0.0399	0.18		*no galaxy*		> 975	...	−16.9
0.0411	0.04		*no galaxy*		> 1002	...	−16.9
0.0454	0.12		*no galaxy*		> 1099	...	−17.2
0.0570	0.06	Obj216	0.0568	−48	1318.9	1.42	−17.7
0.0672	0.12		*no galaxy*		> 1569	...	−18.1
0.1113	0.09	Obj242	0.1116	67	563.2	0.89	−19.2
0.1197	0.04	Obj172	0.1216	508	104.0	4.28	−19.3
0.1214	0.63	Obj172	0.1216	54	104.0	0.46	−19.4

ies brighter than $M \simeq -17.0$. There are $2-3$ published examples of a Lyα line lying in a void between galaxy structures at low-redshift (Shull et al. 1996), and, if the identification of the $z_{\rm abs} = 0.0399$ and 0.0454 systems towards Q1821+643 is correct (see §2.2), then this would be another good example of Lyα lines avoiding galaxies. Of course, at $z \simeq 0.04$, 30 arcmins corresponds to only $1h^{-1}$ Mpc, which makes it possible that galaxies forming part of a loose group at these redshifts might be missed. If we consider galaxies listed in the NED outside our 30 arcmin survey radius, we find only eight nearby galaxies, at large distances of $3.0-10.0\ h^{-1}$ Mpc from the QSO line of sight within a redshift range $z = 0.038-0.042$. Although the catalogue of galaxies from the NED is in no sense complete, (and drawing any inferences from such a catalog may be highly misleading), this does suggest that some Lyα absorbers avoid galaxies on scales of at least a few Mpc.

3.3 Galaxy-absorber correlation functions: are absorbers associated with galaxies?

It is clear from the proceeding section that we need a statistical approach to establishing whether apparent galaxy-absorber correlations are real. In this section, therefore, we calculate the galaxy-galaxy and galaxy-absorber cross-correlation functions in our data set to test the significance of such associations.

We have used the formalism given by Mann, Saunders & Taylor (1996), which for the galaxy-galaxy correlation function reduces to the estimator of $\xi_{\rm gg}$ given by Hamilton (1993). To calculate the galaxy-absorber cross-correlation, $\xi_{\rm gl}$, in redshift space, where separations are denoted as s, we have used their generalization

$$1+\xi_{\rm gl}(s) = \frac{D_gD_l(s)}{D_gR_l(s)}\frac{R_gR_l(s)}{R_gD_l(s)} \quad (1)$$

where $D_gD_l(s)$ is the weighted pair counts of galaxies and lines whose separation places them in a bin centred on s, R_gR_l is the corresponding weighted count for a random catalogue of a) galaxies covering the same area of sky and having the same selection function as the data, and b) lines randomly distributed along the line of sight with a correction for an evolving number density with redshift. D_gR_l, R_gD_l and R_gR_l are the weighted counts of cross pairs between the data and the random catalogs.

For the weighting of the pair counts we adopt the now 'standard' choice of using either $w(r) = 1$ — no weighting — (where r denotes the radial distance of a galaxy/line from the observer) or, for galaxies,

$$w(r,s) = 1/[1+4\pi\phi(r)J_3(s)] \quad (2)$$

(Peebles 1973; Hamilton 1993; Mann, Saunders & Taylor 1996; Tucker et al. 1997). Here, $\phi(r)$ is the selection function, which we take simply to be the number density of galaxies in our survey, $n(r)/V(r)$, as calculated from our data. In this weighting scheme, $J_3(s)$ is defined as

$$J_3(s) \equiv \int_0^s x^2\xi(x)dx \quad (3)$$

and we have used the results from the Las Campanas Redshift Survey (LCRS; Tucker et al. 1996), $\xi(s) = (s_0/s)^\gamma$ with $s_0 = 6.3$ and $\gamma = 1.52$ to evaluate $J_3(s)$. In fact, the correlation function we calculate is relatively insensitive to using this weighting function. For absorption lines, $w(r)$ is always set equal to unity. To ensure the correct number density of lines, random catalogs were generated with the number of lines $n(z) \propto (1+z)^\gamma$, where $\gamma = 0.42$ (Bahcall et al. 1996). Although this is inevitably only an approximation, because we have included Lyα lines with equivalent widths less than the 0.24 Å used to evaluate $n(z)$, the correction has little effect over the small redshift range discussed herein. For all estimates of ξ_{gg} and ξ_{gl}, we have used 10000 points for the random catalogues, and a maximum redshift of $z = 0.2$. For ξ_{gl}, we have used a minimum redshift of 0.0060 for lines and galaxies, since below this, we cannot distinguish Lyα lines from the Damped Lyα line of our own Milky Way.

We first show in Fig. 6 (top) the galaxy auto-correlation function for galaxies weighted in the way described in equation 2. Errors shown are 1σ error bars calculated in the way prescribed by Mo et al. (1992). Also plotted is $1+\xi_{\rm gg}$ from the LCRS (dotted line). The figure shows, unsurprisingly, that the galaxies are clustered in much the same way as seen in more extensive galaxy surveys.

In Fig. 7 we plot the galaxy-absorber correlation function, $\xi_{\rm gl}$. For bins with no galaxies or Lyα clouds detected, we have set $\xi_{\rm gl} = 1$ to indicate the size of bins used to calculate $\xi_{\rm gl}$. In Fig. 7a the correlation is dominated by a single point between $0.36-0.64\ h^{-1}$ Mpc; this is Obj172 lying $104\ h^{-1}$ kpc from the QSO sightline (Table 3) at a redshift of 0.1216. This correlation calculation assumes a (comoving) Hubble flow; hence the difference between $z_{\rm gal}$

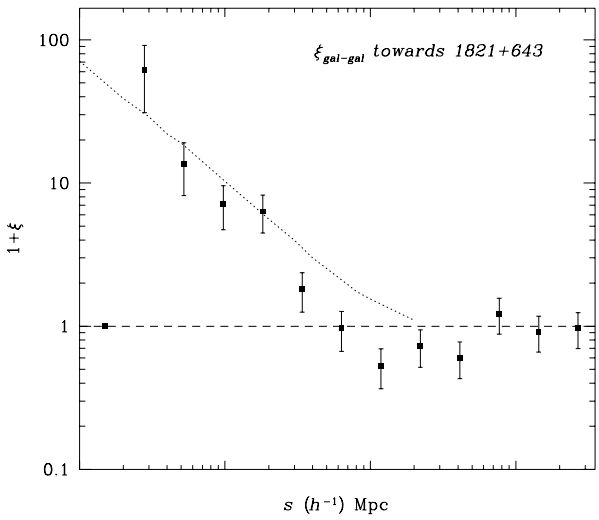

Figure 6. The galaxy auto-correlation function, $\xi_{\rm gg}$, of galaxies in our sample towards Q1821+643. For comparison, the auto-correlation of galaxies found from the Las Camapanas Redshift Survey (Tucker et al. 1997) is shown as a dotted line.

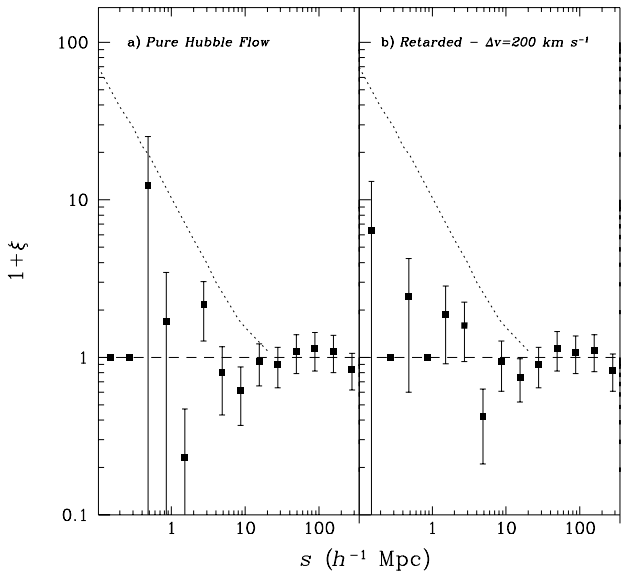

Figure 7. The galaxy-absorber cross-correlation function, $\xi_{\rm gl}$, towards Q1821+643. $\xi_{\rm gl}$ is calculated (a) assuming that values of Δv between absorbers and galaxies arise from the Hubble Flow, and (b) assuming a retarded Hubble Flow such that Δv is set to zero if $\Delta v \leq 200$ km s^{-1}. For comparison, the galaxy-galaxy correlation function found by Tucker et al. (1997) for the LCRS is again shown as a dotted line.

and $z_{\rm abs}$ of $\simeq 0.0002$ means that the distance of galaxy and absorber becomes 518 h^{-1} kpc, even though this value of Δz is within our measurement errors of $z_{\rm gal}$ and $z_{\rm abs}$. Nevertheless, the detection of a galaxy at these impact parameters remains statistically significant; given a random distribution of galaxies and absorbers, we would only have expected 0.02 pairs instead of the one we found. Hence this galaxy-absorber association is unlikely to have arisen by chance. Apart from this pair, Fig. 7a shows that the majority of absorbers are uncorrelated with galaxies, that is, that galaxies at similar redshifts to absorbers on scales of $0.5-2$ h^{-1} Mpc in Fig. 4 probably arise by chance. We note a slight excess between $s = 2.0 - 3.6$ h^{-1} Mpc, but the point is within 2σ of $\xi_{\rm gl} = 0$ (7 pairs were expected, 10 were detected). We note that the lack of any galaxy-absorber pairs at separations of $s = 0.15$ and 0.27 h^{-1} Mpc is not significant: compared with the randomly generated catalogue of galaxies and absorbers, less than 1 galaxy-absorber association was expected for each of these bins.

The problems in taking the projected two-point correlation function and estimating the proper three-dimensional spatial correlation function (Davis & Peebles 1983) for galaxies and absorbers are discussed in detail by M93. It is of more interest, however, to calculate $\xi_{\rm gl}$ using a "retarded Hubble Flow" to take into account the possibility that a galaxy and an absorber may be at the same (radial) distance from us, but have peculiar velocities with respect to each due to the origin of the absorbing gas (e.g. halo gas co-rotating with a galaxy disk). Hence in Fig. 7b we calculate $\xi_{\rm gl}$ with Δv set to zero if the measured value is $|\Delta v| \leq 200$ km s^{-1}, and Δv corrected to $\Delta v - 200$ km s^{-1} if $|\Delta v| > 200$ km s^{-1}. (The resulting correlation is changed little by adopting values of $100 - 300$ km s^{-1} as the criterion for setting $\Delta v = 0$.) The figure shows that in this case, absorbers and galaxies tend to more consistently have values of $\xi_{\rm gl} > 0$. This suggests that absorbers and galaxies are weakly associated if it is *assumed* that the velocity difference is not related to any real physical separation, i.e. if the real separation between galaxy and absorber is the measured value of ρ. However, it is important to realise not only that all the points are within 2σ of $\xi_{\rm gl} = 0$, but that this correlation is sensitive to the exact sample of Lyα lines used; simply removing a line at random from the list to test the robustness of the correlation can remove the apparent consistency of having most of the points with $\xi_{\rm gl} > 0$. This lack of robustness is not surprising given the small sample size of our data set.

We conclude that weak absorbers are uncorrelated, or at best, weakly correlated, with galaxies, on scales of beyond a few hundred h^{-1} kpc or more. Given that there may be more of a significance for the retarded Hubble Flow estimate of $\xi_{\rm gl}$, we can speculate on what this might mean. In what scenarios could galaxies and absorbers be at the same radial distance from us? One possibility is that absorbing gas is directly associated with the identified galaxy. This seems unlikely for points in Fig. 4 and 5 with $\rho = 0.5-2$ h^{-1} Mpc since there is good evidence that individual galaxy halos do not have absorbing gas beyond $\rho = 200 - 300$ h^{-1} kpc (LBTW; BBP). A second possibility is that the gas is a remnant of prior galaxy-galaxy interactions. Although tidal debris is not a favoured explanation for the origin of the $z \sim 0.5$ Mg II absorption lines (see, e.g. Steidel et al. 1994), nearby interacting galaxies have been shown to produce the characteristics of higher redshift Mg II systems (Bowen et al. 1995), while tidal debris as an origin of Lyα absorbers has been discussed by Morris & van den Bergh (1994). This in-

terpretation will remain hard to test, as observing the more subtle signs of galaxy-galaxy interactions is difficult.

Finally, galaxies and absorbers could be at similar distances if they inhabit the same dark matter (DM) structures which constitute the large scale structure (LSS) of the Universe. Many CDM-based numerical simulations (e.g. Cen et al. 1994; Petitjean, Mücket & Kates 1995; Zhang et al. 1995; Mücket et al. 1996) now point to the possibility that low column density H I gas simply follows the same LSS as galaxies (at least at high redshift). It seems likely that galaxies and absorbers which lie in DM sheets and filaments will have small (but non-zero) velocity differences, since the velocity width of galaxy shells seen in local LSS is $200 - 300$ km s^{-1} (e.g. Santiago 1995). Hence the measured values of ρ may well represent real distances between galaxies and absorbers, at least for sheets aligned perpendicular to our line of sight.

3.4 Conclusions and Summary

We have detected a single galaxy 104 h^{-1} kpc from the line of sight of Q1821+643; Lyα absorption arises at the same redshift as the galaxy to within measurement errors. The association is statistically significant compared to a randomly distributed ensemble of clouds and galaxies, suggesting a direct link between absorber and galaxy. The line is strong ($W_r = 0.63$ Å) and its detection is consistent with those of similarly strong lines within 160 h^{-1} kpc of bright galaxies found by LBTW. The next nearest galaxies are 291 h^{-1} kpc and 410 h^{-1} kpc away from the sightline, and these show no absorption to very low equivalent width limits ($W_r < 0.05$ Å) within 600 km s^{-1}. Beyond 500 h^{-1} kpc, several absorption systems are found at similar redshifts to the galaxies, but these coincidences are likely to be accidental.

Five of ten (50%) Lyα absorption systems out to a redshift of 0.12 have no galaxies within 600 km s^{-1} and separations less than $(0.7 - 1.3)$ h^{-1} Mpc. At these redshifts, our magnitude limited redshift survey would have been able to detect at least L^* luminosity galaxies. Excluding the one Lyα system apparently associated with the galaxy described above, two Lyα systems have galaxies within 600 km s^{-1} and $\rho = 0.4 - 0.7$ h^{-1} Mpc, but these associations are again probably coincidental. Eight of the ten lines have *weak* equivalent widths ($W_r < 0.2$ Å), and we conclude that this population is uncorrelated, or at best, weakly correlated, with galaxies. A similar result was found by Stocke et al. (1995) for lines with $W_r \leq 0.1$ Å detected in their own and previously published data sets.

The nature of the strong lines is less clear. The detection of strong lines within 200 h^{-1} kpc of galaxies by LBTW, and the association of one of two strong lines (out to a redshift of 0.12) with a galaxy at a separation of 104 h^{-1} kpc in our own survey supports the idea that strong lines are associated with galaxies while weak ones are intergalactic in origin. This is the 'two-population' explanation proposed by Mo & Morris (1994) and Bahcall et al. (1996). The difficulty in unambiguously drawing this conclusion from our analysis is that our data set contains too few strong lines at low redshift to adequately characterise the nature of this population. Le Brun et al. (1996) have published the only other available survey of the association of strong (FOS-detectable) lines with galaxies; of 13 Lyα systems listed with $W_r > 0.24$ Å, four have galaxies coincident in velocity which are within 200 h^{-1} kpc of a QSO sightline, five are in the range $\rho = 200 - 500$ h^{-1} kpc, and the remaining four are at separations beyond 1.0 h^{-1} Mpc — a roughly even spread in impact parameters. Much of this ambiguity may be down to the 43 % completeness of their survey at $m_r = 18.5$, which ensures considerable difficulty in detecting intermediate brightness galaxies at the redshifts of the Lyα systems studied, $z_{\rm abs} = 0.09 - 0.77$. However, detection of even a few bright galaxies so close to Lyα systems may suggest that strong lines are directly associated with galaxies. Clearly, to explore this possibility further, more complete galaxy surveys are required at the redshifts of strong lines. A second approach would be to directly search for Lyα absorption in halos of nearby, isolated galaxies at impact parameters of $0 - 500$ h^{-1} kpc.

Our results do not rule out the possibility that strong Lyα lines are directly associated with galaxies of *all* luminosities — including faint dwarf galaxies which have not been found in the surveys described above — on scales of a few hundred h^{-1} kpc. This would explain why it has been easy to find some absorbing galaxies (i.e. the bright ones) while some strong lines appear to have no associated galaxies (those which are too faint to be detected). Only Rauch et al. (1996) have searched for low surface brightness galaxies which might be responsible for Lyα absorption lines toward 3C 273, and none were detected, although two faint galaxies (CGCG014−054, $M_B = -16.2$ and the H I cloud H I 1225+01, $M_B = -14.0$) are at similar redshifts to the lowest redshifted Lyα lines at 1012 and 1582 km s^{-1} and within $\rho = 200$ h^{-1} kpc. BBP also found Lyα absorption toward Q1001+2910 at the same velocity as UGCA201 ($M_B = -16.2$, $\rho = 117$ h^{-1} kpc) with no other galaxies nearby. Unfortunately, it is hard to test whether these coincidences are accidental or not.

The amount of data needed to fully understand the origin of the Lyα-forest is still far from available. Obtaining high quality, high resolution *HST* spectra toward Q1821+643 demonstrates the importance of such data, not only for exploring the weak population of Lyα lines, but simply in disentangling the Lyα-forest from Galactic absorption lines when working at low-redshift. The nature of the strong lines remains unclear, and as mentioned above, a direct search for Lyα lines within a few hundred h^{-1} kpc of nearby, isolated galaxies would provide much needed information as to whether strong lines alone are directly associated with galaxies.

ACKNOWLEDGMENTS

It is a pleasure to thank Andy Taylor, Licia Verde, and John Peacock for highly illuminating discussions. We are also very grateful to Mike Irwin for providing candidate objects in the field of Q1821+643 from APM scans. IRAF is distributed by the National Optical Astronomy Observatories, which is operated by the Association of Universities for Research in Astronomy, Inc., under cooperative agreement with the National Science Foundation. The NASA/IPAC Extragalactic Database (NED) is operated by the Jet Propulsion Labo-

ratory, Caltech, under contract with National Aeronautics and Space Administration.

REFERENCES

Bahcall, J. N., Jannuzi, B. T., Schneider, D. P., Hartig, G. F., Bohlin, R., & Junkkarinen, V. 1991, ApJL, 377, L5
Bahcall, J. N., Jannuzi, B. T., Schneider, D. P., Hartig, G. F., & Green, R. F. 1992, ApJ, 397, 68 (B92)
Bahcall, J. N., et al. 1993, ApJS, 87, 1 (KPI)
Bahcall, J. N., et al. 1996, ApJ, 457, 19
Bowen. D. V., & Blades, J. C., & Pettini, M. 1996, ApJ, 464, 141 (BBP)
Bowen, D. V., & Blades, J. C., & Pettini, M. 1995, ApJ, 448, 634
Cen, R., Miralda-Escudé, J., Ostriker, J. P., & Rauch, M. 1994, ApJ, 437, L9
Davis, M., & Peebles, P. J. E. 1983, ApJ, 267, 465
Hamilton, J. A. S. 1993, ApJ, 417, 19
Lanzetta, K. M., Bowen, D. V., Tytler, D., & Webb, J. K. 1995, ApJ, 442, 538, 1995 (LBTW)
Lanzetta, K. M., Webb, J. K., & Barcons, X. 1996, ApJ, L17
Lockman, F. J., & Savage, B. D. 1995, ApJS, 97, 1
Le Brun, V., Bergeron, J., & Boissé P. 1996, A&A, 306, 691
Lewis, J. 1996, WYFFOS data reduction handbook, RGO.
Mann, R. G., Saunders, W., & Taylor, A. N. 1996, MNRAS, 279, 636
Mo, H. J., Jung, Y. P., & Börner, G. 1992, ApJ, 392, 452
Mo, H. J.. & Morris, S. L. 1994, MNRAS, 269, 52
Morris, S. L., Weymann, R. J., Savage, B. D., & Gilliland, R. L. 1991, ApJL, 377, L21
Morris, S. L., Weymann, R. J., Dressler, P. J., McCarthy, P. J., Smith, B. A., Terrile, R. J., Giovanelli, R., & Irwin, M. 1993, ApJ, 419, 524 (M93)
Morris, S. L., & van den Bergh, 1994, ApJ, 427, 696
Mücket, J. P., Petitjean, P., Kates, R. E., & Riediger, R. 1996, A&A, 308, 17.
Peebles, P. J. E. 1973, ApJ, 185, 413
Petitjean, P., Mücket, J. P., & Kates, R. E., 1995, A&A, 295, L9
Rauch, M., Weymann, R. J., & Morris, S. L. 1996, ApJ, 458, 518
Santiago, B. 1995, in Wide Field Spectroscopy and the Distant Universe, proceedings of the 35th HErstmonceux Conference, eds. Maddox., S. J. & Aragón-Salamanca, A., pg 81
Sargent, W. L. W., Young, P. J., Boksenberg, A., & Tytler, D. 1980, ApJS, 42, 41
Savage, B. D., Sembach, K. R., & Lu, L. 1995, ApJ, 449, 145 (SSL)
Schneider, D. P., Bahcall, J. N., Gunn, J. E., & Dressler, A. 1992, AJ, 103, 1047
Shull, J. M., Stocke, J. T., & Penton, S. 1996, AJ, 111, 72
Steidel, C. C., Dickinson, M., & Persson 1994, ApJL, 437, L75
Stocke, J. T., Shull, J. M., Penton, S., Donahue, M., & Carilli, C., 1995, ApJ, 451, 24
Tripp, T., Lu, L., & Savage, B. D. 1997, poster paper at the 13th IAP Meeting, Structure & Evolution of the Intergalactic Medium from QSO Absorption Line Systems.
Tucker, D. L. et al. 1997, MNRAS, in press
Valdes, F. 1992, Guide to the HYDRA Reduction Task DOHYDRA, IRAF Group - Central Computer Services, NOAO.
Young, P. J., Sargent, W. L. W., Boksenberg, A., Carswell, R. F., & Whelan, J. A. J. 1979, ApJ, 229, 891
Zhang, Y., Anninos, P., Norman, M. L. 1995, ApJ, 453, L57